

Experimental investigation of self-starting operation in a F8L based on a symmetrical NOLM

B. Ibarra-Escamilla ^{a,*}, O. Pottiez ^b, E.A. Kuzin ^a, J.W. Haus ^c,
R. Grajales-Coutiño ^a, P. Zaca-Moran ^d

^a *Instituto Nacional de Astrofísica, Óptica y Electrónica, Departamento de Óptica, A.P. 51 y 216, Puebla, Pue 72000, Mexico*

^b *Centro de Investigaciones en Óptica, Loma del Bosque 115, Col. Loma del Campestre, León, Gto 37150, Mexico*

^c *Electro-Optics Program, The University of Dayton, Dayton, OH 45469, USA*

^d *Benemerita Universidad Autónoma de Puebla, Instituto de Ciencias, A.P. 207, Puebla, Pue 72000, Mexico*

Received 18 July 2007; received in revised form 29 October 2007; accepted 29 October 2007

Abstract

We experimentally analyze the self-starting operation of a figure-eight mode-locked fiber laser. The design is based on a power-balanced nonlinear optical loop mirror (NOLM) with highly twisted low-birefringence fiber and a quarter-wave (QW) retarder in the loop. The NOLM operates by nonlinear polarization rotation. Self-starting mode-locking requires a careful adjustment of the NOLM low-power transmission, which is easily realized with our setup by adjusting the angle of the QW retarder. The laser is capable of generating ~ 20 ps pulses at the fundamental repetition frequency of 0.78 MHz.

© 2007 Elsevier B.V. All rights reserved.

PACS: 07.60.Vg; 42.55.Wd; 42.60.Fc; 42.81.Wg

Keywords: Sagnac interferometer; Fiber lasers; Mode-locking fiber lasers; Fiber-optic devices

1. Introduction

Nonlinear optical loop mirrors (NOLMs) [1] are very versatile devices that have been investigated for various applications including optical switching, demultiplexing, phase conjugation, and passive mode-locking of fiber lasers. In most cases, the NOLM is formed by an asymmetrical coupler whose output ports are connected to form a loop. In the loop there are thus two counter-propagating beams traveling in opposite directions with different powers. This power imbalance causes a difference in the nonlinear phase shifts of these beams. This results in an intensity-dependent transmission (switching) characteristic of the NOLM. The polarization in many cases is not controlled carefully. In some cases however highly birefrin-

gence fiber maintaining linear polarization are used. In that case the polarization of the beams does not contribute to switching. If now we use a symmetrical coupler in the loop, switching can still be obtained, however, through the polarization dependence of the phase shift. It is then necessary to create a polarization asymmetry between the counter-propagating beams. In our previous investigation we studied a scheme including a symmetrical coupler, highly twisted low-birefringence fiber and a quarter-wave (QW) retarder in the loop to break the polarization symmetry [2]. High twist is applied to reduce the fiber residual birefringence, which will vary with environmental conditions and is a contributor to unstable NOLM behavior. Actually, it was shown in Ref. [3] that twisted fiber behaves like an ideal isotropic fiber. By dominating over the residual birefringence, the circular birefringence imposed by twist (optical activity) substantially improves the robustness of the device, as demonstrated in a previous paper [4].

* Corresponding author. Tel./fax: +52 222 247 2940.

E-mail address: baldemar@inaoep.mx (B. Ibarra-Escamilla).

through the couple PC-P1) the NOLM output polarization component that is orthogonal to the NOLM input polarization. The proposed setup is very similar to, but still different from the one used in a previous study (Ref. [7]), in which mode-locking was not self-starting as it required an external stimulation.

In this new experimental setup we demonstrate that the self-starting passive mode-locking operation of a F8L can be obtained through simple and clear adjustments to have desirable low power transmission and nonlinearity. The necessary adjustment is achieved by the rotation of the QW1 retarder in the NOLM loop. Self-starting mode-locking critically depends on the precise adjustment of the NOLM. We determined the QW1 retarder angle required for self-starting operation. Additional elements playing a key role in the self-starting capability of the present setup are the FBG as a filtering element and the MDT718-125 fiber rotators FR1 and FR2 included in the Coupler 1 output arms. The fiber rotators allow fine adjustment of the NOLM low-power transmission and their effect on the self-starting operation will be explained below.

On the other hand, the role of the FBG is quite complex. Although recent studies show that the filtering element can play a crucial role in the mode-locking mechanism [19], its main purpose here is to reduce the ASE noise in the laser. As shown in Ref. [18], an interesting aspect of the self-starting problem in mode-locking is the dual role that noise plays in the mode-locking process: enabling the potential barrier between the continuous-wave (cw) and mode-locked states to be stochastically overcome, and the noisy operation of the laser in the mode-locked state. The fluctuations need to be strong enough to eventually “kick” the laser out of the metastable cw state to the more stable mode-locked state. Hence, by reducing intracavity noise, the FBG reduces the strength of the fluctuations which are needed to overcome this barrier. However, the FBG high-frequency filtering still retains enough lower frequency noise in the cavity for self-starting of our laser. Reducing intracavity noise also tends to stabilize the mode-locking state of operation of the laser. Finally, the FBG rejects the side lobes in the spectrum that appear due to modulation instability. Although modulation instability is not inconsistent with pulse formation and self-starting mode-locking, in our particular case suppressing the side lobes may help to avoid the break up of the picosecond pulse, and thus to maintain single-pulse operation. We experimentally found that the FBG creates favorable conditions for self-starting in our configuration.

We demonstrated in a previous paper [8] that by selecting the NOLM output polarization parallel to the input polarization, we have low-power transmission equal to zero at any angle of the QW1 retarder. By contrast, when the orthogonal component is selected, the value of low-power transmission depends on the QW1 position, as shown in Fig. 2. Through the QW1 orientation it is possible to change the transmission at low input power from a maximum (80%) to a minimum (0%) (see Fig. 2a). The trans-

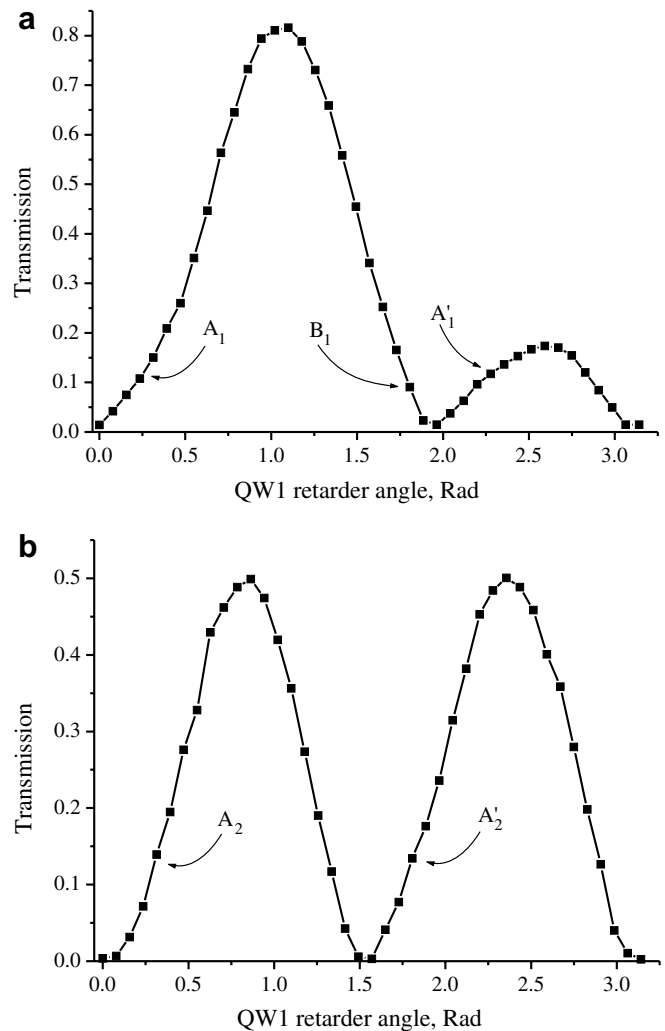


Fig. 2. Low-power transmission amplitude dependence on the QW1 retarder angle when two peaks in a period of π rad: (a) have different amplitudes and (b) have similar amplitudes.

mission plot in Fig. 2a exhibits two peaks in a period of π rad, whose amplitudes are substantially different. Maximum low-power transmission can be adjusted easily, between 50% (see Fig. 2b) and 100%, by adjusting the birefringence of the Coupler 1 output arms. This can be done in practice by twisting and pressing the fiber arms using the MDT718-125 fiber rotators FR1 and FR2 [20]. The inclusion of these elements in our setup thus allows a precise control of the birefringence of the Coupler 1 output arms, and thus of the low-power transmission, which is crucial for self-starting mode-locking, as it will appear from our experimental results.

We found the self-starting mode-locking when the position of the QW1 is around the point A_1 for the transmission presented on the Fig. 2a. As we can see in this figure, the transmission at point A_1 is around 11%. In the case of self-starting mode-locked pulses, the transmission is increased to 22%. At this point A_1 , when the pump power is greater than 70 mW, we get self-starting mode-locked

pulses. In the similar point A'_1 on the Fig. 2a the self-starting operation was not found. When the two peaks have similar amplitudes for low-power transmission (see Fig. 2b), the nonlinear transmission for points A_2 and A'_2 (dashed with circles curve in Fig. 3) are the same, and in these conditions we found the self-starting mode-locked operation in both positions. From these observations and others we conjecture that self-starting mode-locked laser operation requires a low-power transmission amplitude that is different from zero.

Fig. 3 shows the simulated nonlinear transmission characteristic of the NOLM for different positions (solid curve represents point A_1 , solid with circles curve represents point B_1 and dashed curve represents point A'_1) of the QW1 retarder when we have different amplitudes of the two peaks for low-power transmission (see Fig. 2a). The self-starting mode-locked operation was possible only at point A_1 . As we can see in Fig. 2a, in terms of low-power transmission, point B_1 is similar to point A_1 . However, these two points lead to distinct nonlinear dependence of the NOLM transmission. At point A_1 (see solid curve in Fig. 3), the nonlinear transmission increases with the input power whereas at point B_1 (see solid with circles curve in Fig. 3) the nonlinear transmission first decreases to zero before it starts to increase. At B_1 it was not possible to observe self-starting mode-locking. The explanation of this situation is quite clear: as intracavity power grows, it first suffers from growing losses through the NOLM, until at some point it cannot spontaneously grow any further, as losses become higher than the gain. A similar nonlinear behavior is observed in the second peak in Fig. 2a (point A'_1), however in this case the values of nonlinear transmis-

sion are smaller (see dashed curve in Fig. 3). In this case cavity losses are higher for the pulses. The self-starting mode-locking was not observed at this point either, probably because the required pump power is higher at point A'_1 than at point A_1 (in our experiment available pump power was limited to 100 mW), in spite of the lower value of critical power at point A'_1 .

Fig. 4 shows the laser output pulses measured by a 10 GHz fast detector and a 20 GHz sampling oscilloscope. Although the short pulse can not be precisely resolved in this measurement, these data were used to simulate the autocorrelation trace (inset in Fig. 4). Self-starting mode-locking appears when pump power is around 70 mW. Mode-locking is maintained if we decrease the pump power down to 20 mW. The scope trace consists of a 30 ps peak and a long tail. We demonstrated that this tail is part of the pulse and not an artifact of the detector [21]. When the pump power is decreased below 20 mW, mode-locking disappears. The pulse repetition frequency is 0.78 MHz. The average power at output 2 is 1 mW for a pump power of 70 mW, giving 5.66 mW of average power entering the NOLM. The optical spectrum of the pulses is shown in Fig. 5, where solid curve is the spectrum for mode-locked operation and dashed curve is the spectrum for cw operation. We centered the spectrum at the maximum of the broad band line. The cw measured spectrum is centered at the FBG maximum wavelength at 1548 nm. This figure reveals a sharp spike (peak a) along with the broad spectrum of the mode-locked signal. This spike is found to occur at specific frequencies, independently of the QW1 retarder angle. The presence of a frequency-shifted narrow-band peak (a) in our case most probably is due to the tail after the peak. We attribute the narrow-band peak to spurious cw oscillation associated with the long tail of the pulse, which contains a substantial part of the pulse energy. The cw spectrum is not stable and fluctuates

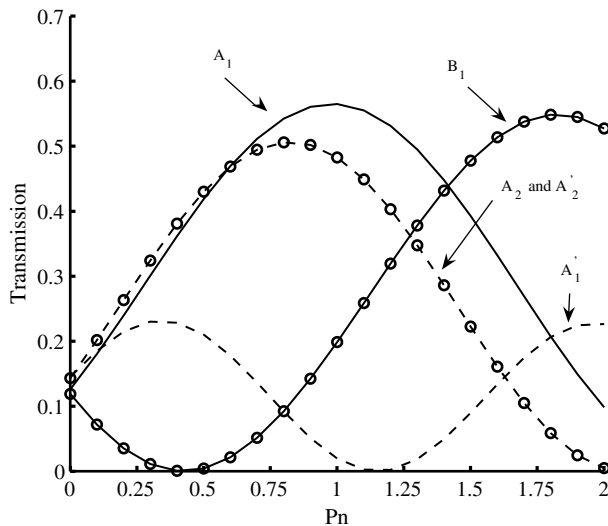


Fig. 3. Nonlinear transmission as a function of the normalized input power P_n . The solid curve corresponds to point A_1 , the solid with circles curve corresponds to point B_1 , and the dashed curve corresponds to point A'_1 when the two peaks have different amplitudes in Fig. 2a. The dashed curve with circles corresponds to points A_2 and A'_2 when the two peaks have similar amplitudes in Fig. 2b. Considering standard single-mode fibers, the value $P_n = 1$ represents about 50–100 W at the NOLM input.

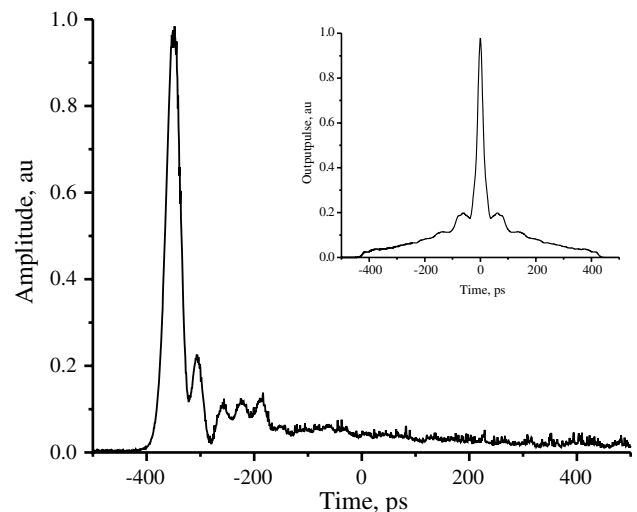


Fig. 4. Pulse waveform monitored with a high-speed photodetector. The inset is the autocorrelation trace calculated using the data of the measured pulse.

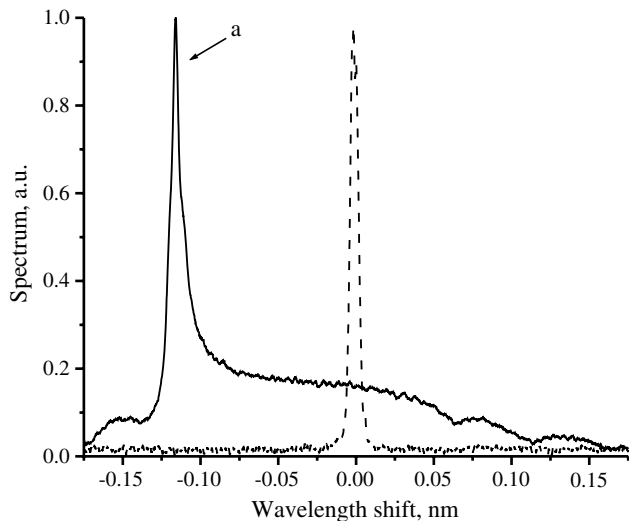


Fig. 5. Optical spectrum from the self-starting, passively mode-locked fiber laser. The solid curve is the spectrum for mode-locked operation, and the dashed curve is the spectrum for cw operation.

around the maximum of the mode-locked spectrum. The full width at half maximum (FWHM) spectrum bandwidth of the mode-locked signal is $\Delta\lambda = 0.19$ nm. The autocorrelation function of the output pulses measured by a FR-103XL autocorrelator is plotted in Fig. 6. The autocorrelator has a time window of about 200 ps. To extend the time range of the autocorrelation function we adjusted the peak at the cut of the window and measured the half of the autocorrelation function. The complete autocorrelation function was reconstructed using the fact that the autocorrelation function is always symmetrical. This figure is in good qualitative agreement with the simulation inset in Fig. 4, showing a wide pedestal that is related to the tail appearing in the waveform. The FWHM of the autocorrelation trace is about 30 ps corresponding to a FWHM pulse duration $\Delta\tau = 21.21$ ps (if a Gaussian profile is

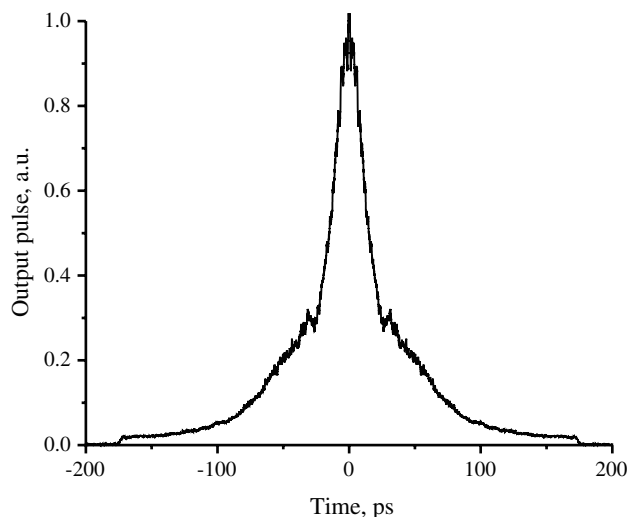


Fig. 6. Measured autocorrelation trace of the output pulses.

assumed) giving $\Delta\nu\Delta\tau = 0.504$ where $\Delta\nu$ is FWHM of the frequency spectrum. This value is close to the value expected for transform-limited pulse shapes, indicating that the pulse has a low chirp.

3. Discussion of the results

The present F8L includes a NOLM with a symmetrical coupler, highly twisted fiber in the loop, and a quarter-wave (QW1) retarder to break the polarization symmetry. Previously, we demonstrated switching through the polarization dependence of the phase shift with this NOLM and, in this paper, we verified its application in a mode-locked laser design. For this goal we inserted a polarizer into the cavity, which is unnecessary for the laser operation, but enables the selection of the polarization component orthogonal to the input at the NOLM output. Under these conditions, the nonlinear transmission of the NOLM+P1 combination is particularly attractive for mode-locking operation. The present laser has the advantages that self-starting mode-locking can be observed by adjusting only one element, the QW1 retarder in the NOLM, in a very clear and repeatable way. The adjustment procedure is straightforward, the QW1 retarder must be around the positions A_1 in Fig. 2. After that, we only have to increase the pump power up to 70 mW to get the self-starting mode-locking operation. When we decrease the pump power until 20 mW, the laser still supports mode-locked pulses in the cavity.

In Fig. 2a the two peaks have different amplitudes. It is possible to adjust the birefringence of the Coupler 1 output arms (using FR1 and FR2) to have two similar peaks reaching around 50% of maximal low-power transmission (in theory, this occurs when the birefringence in the fiber arms is cancelled, Fig. 2b). Fig. 7a shows the simulated transmission characteristic of the NOLM for different positions of the QW1 retarder in the region around point A_1 in Fig. 2a (nonlinear transmission at point A_1 is represented by the dashed curve). As we can see in Fig. 7a, when the low-power transmission is too high (say $>50\%$), the nonlinear dependence is mainly decreasing with power (see solid with circles curve). This intensity-limiting action of course does not favor mode-locking. On the other hand, if low-power transmission is too small (i.e. close to zero), then nearly all low-power oscillation is absorbed by the NOLM and the laser can not initiate, at least without an external stimulation. At intermediate points like A_1 , transmission grows substantially with power, so that saturable absorber action is obtained, which allows mode-locking, whereas low-power transmission is still different from zero, making initial lasing possible. It is then understandable that, if intracavity power is sufficient, random positive fluctuations of the power level will be favored through the NOLM, and grow, leading to spontaneous pulse formation, or self-starting mode-locking. Self-starting mode-locking thus requires a precise adjustment of the NOLM low-power transmission, which is easily realized with our setup with the QW1 retarder.

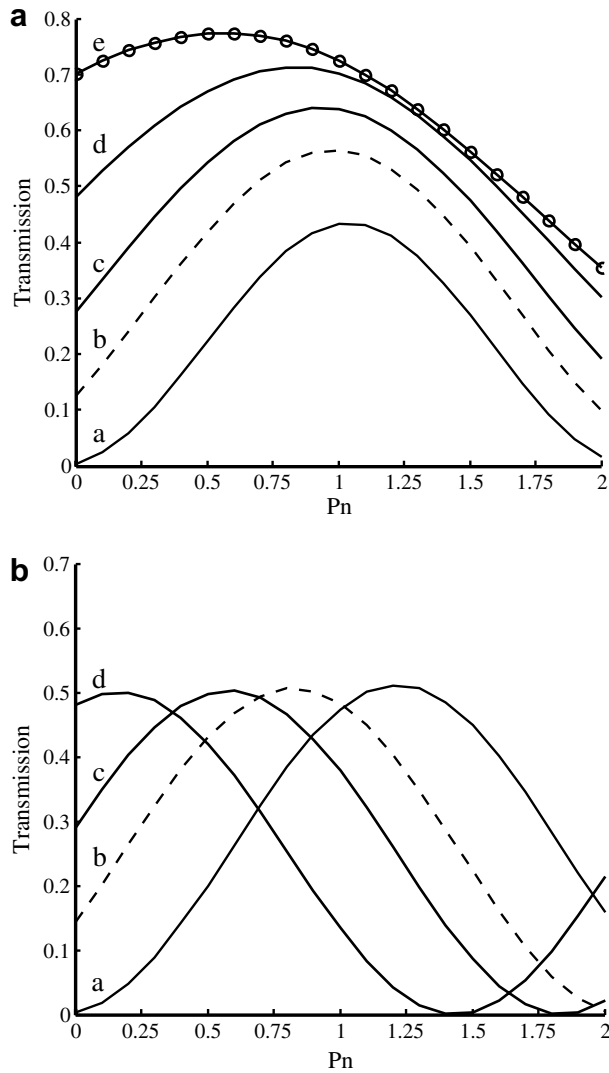


Fig. 7. Nonlinear transmission in function of the normalized input power P_n for different positions of the QW1 retarder in the region around points: (a) A_1 when the two peaks have different amplitudes as in Fig. 2a (QW1 retarder angle = 0, 0.25, 0.5, 0.7 and 0.8 rad, from a to e, respectively); and (b) A_2 when the two peaks have similar amplitudes as in Fig. 2b (QW1 retarder angle = 0, 0.3, 0.5 and 0.75 rad, from a to d, respectively). The dashed curves correspond to points A_1 and A_2 in both cases. The solid line with circles corresponds to a QW1 position for which the low-power transmission is too high (>50%). Considering standard single-mode fiber, $P_n = 1$ represents about 50–100 W at the NOLM input.

Fig. 7b displays the simulated nonlinear transmission characteristics of the NOLM for different positions of the QW1 retarder, when the two peaks are similar, as in Fig. 2b, the NOLM transmission at point A_2 is represented by the dashed curve. Self-starting mode-locking is still observed for about the same positions of QW1 (point A_2 in Fig. 2b), however more pump power (90 mW) is required. The higher pump power requirement could be related to the lower values of nonlinear transmission of the NOLM obtained when maximum low-power transmission is decreased, as shown in Fig. 7 by comparing (b) and (a) curves. However the values of maximal nonlinear trans-

mission at points A_1 and A_2 (dashed curves) are not substantially different, according to the simulation. We also investigated the laser operation at point A_2' after adjusting the Coupler 1 output arms birefringence (with the adjustment of FR1 and FR2) to have nearly equal peak amplitudes in Fig. 2b. The simulations showed that a nonlinear characteristic very similar to the dashed curve of Fig. 7b is obtained in this case, and the self-starting mode-locking was observed at this point in the same conditions as at point A_2 . The stability of the laser is limited by environmental effects on the fiber, which over days required some minor adjustments of the QW1 retarder.

4. Conclusions

In conclusion, we experimentally demonstrate the operation of a self-starting mode-locked figure-eight fiber laser based on a symmetrical NOLM with a highly twisted low-birefringence fiber and a quarter-wave (QW) retarder in the loop. The mode-locking operation is achieved by the polarization dependence of the phase shift in the NOLM. Self-starting mode-locking requires a careful adjustment of the NOLM low-power transmission, which is easily realized with our setup by adjusting the angle of the QW retarder. The pulse repetition frequency is 0.78 MHz. The FWHM of the autocorrelation function is 30 ps. The adjustment procedure is straightforward. We achieved stable generation of picosecond pulses with milliwatts of average output power.

Acknowledgement

E.A.K. was supported by CONACYT Grant 47169, O.P. was supported by CONCYTEG Grant 07-04-K662-043.

References

- [1] N.J. Doran, D. Wood, *Opt. Lett.* 13 (1988) 56.
- [2] O. Pottiez, E.A. Kuzin, B. Ibarra-Escamilla, F. Mendez-Martinez, *Opt. Commun.* 254 (2005) 152.
- [3] T. Tanemura, K. Kikuchi, *J. Lightwave Technol.* 24 (2006) 4108.
- [4] O. Pottiez, E.A. Kuzin, B. Ibarra-Escamilla, F. Mendez-Martinez, *Opt. Commun.* 229 (2004) 147.
- [5] I.N. Duling III, M.L. Dennis, *Compact Sources of Ultrashort Pulses*, Cambridge University Press, Cambridge, 1995.
- [6] J.W. Haus, G. Shaulov, E.A. Kuzin, J. Sanchez-Mondragon, *Opt. Lett.* 24 (1999) 376.
- [7] E.A. Kuzin, B. Ibarra-Escamilla, D.E. Garcia-Gomez, J.W. Haus, *Opt. Lett.* 26 (2001) 1559.
- [8] B. Ibarra-Escamilla, E.A. Kuzin, P. Zaca-Morán, R. Grajales-Coutiño, F. Mendez-Martinez, O. Pottiez, R. Rojas-Laguna, J.W. Haus, *Opt. Express* 13 (2005) 10760.
- [9] H.A. Haus, E.P. Ippen, *Opt. Lett.* 16 (1991) 1331.
- [10] F. Krausz, T. Brabec, CH. Spielmann, *Opt. Lett.* 16 (1991) 235.
- [11] J. Herrmann, *Opt. Commun.* 98 (1993) 111.
- [12] D.J. Richardson, R.I. Laming, D.N. Payne, V. Matsas, M.W. Phillips, *Electron. Lett.* 27 (1991) 542.
- [13] H.A. Haus, E.P. Ippen, K. Tamura, *IEEE J. Quantum Electron.* 30 (1994) 200.

- [14] C.J. Chen, P.K.A. Wai, C.R. Menyuk, *Opt. Lett.* 20 (1995) 350.
- [15] A.B. Grudinin, S. Gray, *J. Opt. Soc. Am. B* 14 (1997) 144.
- [16] A. Gordon, B. Fischer, *Opt. Lett.* 28 (2003) 1326.
- [17] A. Gordon, B. Vodonos, V. Smulakovsky, B. Fischer, *Opt. Express* 11 (2003) 3418.
- [18] B. Vodonos, A. Bekker, V. Smulakovsky, A. Gordon, O. Gat, N.K. Berger, B. Fischer, *Opt. Lett.* 30 (2005) 2787.
- [19] A. Chong, J. Buckely, W. Renniger, F. Wise, *Opt. Express* 14 (2006) 10095.
- [20] B. Ibarra-Escamilla, E.A. Kuzin, O. Pottiez, J.W. Haus, F. Gutierrez-Zainos, R. Grajales-Coutiño, P. Zaca-Moran, *Opt. Commun.* 242 (2004) 191.
- [21] O. Pottiez, E.A. Kuzin, B. Ibarra-Escamilla, *IEEE Photon. Technol. Lett.* 19 (2007) 1347.